Acta Pharm. **73** (2023) 341–362
https://doi.org/10.2478/acph-2023-0031

Original research paper

Synthesis and protective effect of pyrazole conjugated imidazo[1,2-*a*]pyrazine derivatives against acute lung injury in sepsis rats *via* attenuation of NF-κB, oxidative stress, and apoptosis

BINBIN ZANG*
LIHUI WANG

The Emergency Department, Henan Province Hospital of TCMThe Second Affiliated Hospital of Henan University of TCM, Zhengzhou City Henan Province, 450002, China

ABSTRACT

The current work was conducted to elucidate the pharmacological effect of pyrazole-conjugated imidazo[1,2-*a*]pyrazine derivatives against acute lung injury in rats in sepsis and their mechanism of action. Various pyrazole-conjugated imidazo[1,2-*a*]-pyrazine derivatives have been synthesized in a straightforward synthetic route. They exhibited a diverse range of inhibitory activity against NF-κB with IC_{50} ranging from 1 to 94 μmol L^{-1}. Among them, compound **3h** [(4-(4-((4-hydroxyphenyl)sulfonyl) phenyl)-5-(4-methoxyphenyl)-4,5-dihydro-1*H*-pyrazol-1-yl) (8-(methylamino)imidazo[1,2-*a*]pyrazin-2-yl)methanone] was identified as the most potent NF-κB inhibitor with IC_{50} of 1.02 μmol L^{-1}. None of the synthesized compounds was found cytotoxic to normal cell-line MCF-12A. The pharmacological activity of the most potent NF-κB inhibitor **3h** was also investigated in cecal ligation and puncture (CLP)-induced sepsis injury of the lung in rats. Compound **3h** was administered to rats after induction of lung sepsis, and various biochemical parameters were measured. Results suggested that compound **3h** significantly reduced lung inflammation and membrane permeability, as evidenced by H&E staining of lung tissues. It substantially reduced the generation of pro-inflammatory cytokines (TNF-α, IL-1B, IL-6) and oxidative stress (MPO, MDA, SOD). It showed attenuation of NF-κB and apoptosis in Western blot and annexin-PI assay, resp. Compound **3h** also reduced the production of bronchoalveolar lavage fluid from the lung and provided a protective effect against lung injury. Our study showed the pharmacological significance of pyrazole-conjugated imidazo[1,2-*a*] pyrazine derivative **3h** against acute lung injury in sepsis rats.

Keywords: pyrazole-conjugated imidazo[1,2-*a*]pyrazine derivatives, synthesis, rats, sepsis, NF-κB, inflammation, oxidative stress, apoptosis

Accepted June 14, 2023
Published online June 15, 2023

*Correspondence; e-mail: 15803849673m@sina.cn

The impaired defense system poses a significant risk to humans, being responsible for grave mortality and morbidity (1). It leads to various diseases, and among them, sepsis is one of the diseases which leads to multiple organ failures and subsequent shock and death. It arises due to infection and provokes the generation of various inflammatory mediators due to complex, intriguing cross-talk between the host and infectious agents. Despite extensive research, treating sepsis and septic shock has remained elusive due to its multifaceted pathophysiology (2). Thus, novel agents are urgently needed that could be able to have multi-target action.

The lung is the most vulnerable organ at several junctures in sepsis, and approximately 25 to 50 % of patients with sepsis may result into acute lung injury (ALI) (3). ALI and its most stern variety, acute respiratory distress syndrome (ARDS), is an inflammatory syndrome of the respiratory system. The rapid onset of respiratory system failure arises from the direct or indirect insult of the lung vasculature system. The mechanism by which ALI hampered the functioning of the lungs includes one or more of the given reasons, such as an increase in the inflammatory response, enhanced infiltration of leukocytes, leakage of protein, and an increase in oxidative stress in the lungs (4). Inflammation is the characteristic hallmark of ALI, and studies have shown that NF-κB is the vital mediator of the inflammatory cascade in ALI (5, 6). Thus, compounds or agents that inhibit these pathological conditions may benefit sepsis-induced ALI.

Because of their extensive biological activity, pyrazole derivatives hold a special place in medicinal chemistry (7). Celecoxib is a successful anti-inflammatory agent currently in clinical practice and belongs to the category of pyrazole scaffolds. Consequently, various pyrazole derivatives were developed as anti-inflammatory agents (8, 9). Numerous studies have also reported the NF-κB inhibitory activity of pyrazole derivatives in multiple models (10).

The NF-κB has been depicted as a critical regulator for developing sepsis-induced organ failure by producing numerous immunomodulatory mediators (11, 12). Studies have shown that this process has been initiated by the translocation of NF-κB to the nucleus from the cytoplasm *via* induction of toll-like receptors (TLRs), such as TLR2 and TLR4, by bacterial products or cytokine receptors, including those for tumor necrosis factor (TNF)-α and interleukin (IL)-1 (13, 14). It led to the activation of NF-κB and promoted the transcription of various genes responsible for inflammation development and progression associated with lung sepsis. Thus, inhibition of NF-κB is a much sought therapeutic strategy to prevent the inflammatory response generated during sepsis-induced lung injury, thereby protecting the lung.

Imidazo[1,2-*a*]pyrazine, another pharmacophore, showed potent anti-inflammatory action (15, 16). However, no study has reported the anti-inflammatory effect of a hybrid derivative of these pharmacophores against sepsis. Thus, in the current study, we aimed to develop a conjugate of pyrazole with imidazo[1,2-*a*]pyrazine in a search for a novel molecule against ALI and its mechanism of action.

EXPERIMENTAL

Chemistry

Starting materials and all other reagents were purchased from Sigma Aldrich (USA). All solvents were of analytical grade and purchased from the Tianjin Hongyan chemical

reagents factory (China). Silica gel for column chromatography (0.053–0.075 mm) was purchased from the Tsingtao Haiyang silica gel desiccant factory (China). Solvents were dried according to standard procedures. Nuclear magnetic resonance spectra (NMR) were recorded on a Bruker Avance 400 instrument (^{1}H NMR at 400 MHz, ^{13}C NMR at 100 MHz) using dimethyl sulfoxide (DMSO-d_6) as a solvent and tetramethylsilane (TMS) as the internal standard. The FTIR spectra were recorded on PerkinElmer 1600 – Series (Perkin Elmer, USA) spectrophotometer. High-resolution mass spectra were acquired on a VG-AUTO SPEC-3000 (Waters, USA) spectrometer. Elemental analysis was performed on a 2400 CHNSO Perkin-Elmer (USA) analyzer.

Synthesis of 8-(methylamino)imidazo[1,2-*a*]pyrazine-2-carbohydrazide (**1**) and various chalcones (**2a–j**) was performed as per the previously reported procedures (17, 18). Initially, hydrazine hydrate, 97 % (0.01 mmol) was poured into a solution of ethyl 8-(methylamino) imidazo[1,2-*a*]pyrazine-2-carboxylate (0.01 mmol) in ethanol (95 %, 30 mL) and refluxed for 5 h. After cooling, the precipitate was filtered, rinsed with water, dried, and crystallized from ethanol. In the next step, chalcones **2a–j** were synthesized by using corresponding acetophenones (0.01 mol) and 4-methoxy benzaldehyde (0.01 mol) in 20 mL ethanol. The reaction mixture temperature was maintained at 20–25 °C for 5–6 hours, and 10 mL of 10 % sodium hydroxide solution was added dropwise while stirring vigorously. To neutralize the reaction mixture, 0.1 mol L^{-1} HCl was used. The intermediate chalcone derivatives **2a-j** were precipitated, filtered, dried, and recrystallized from ethanol, as shown in Scheme 1.

Synthesis of ***4a–j****. General procedure*. – The 8-(methylamino)imidazo[1,2-*a*]pyrazine-2-carbohydrazide (**1**) (10 mmol) and chalcone derivative **2a–j** (10 mmol) were refluxed for

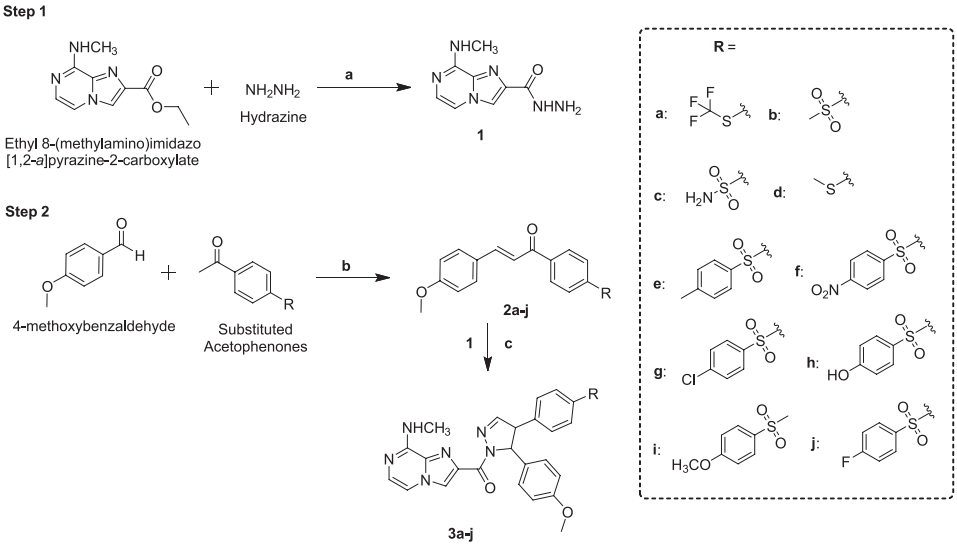

Scheme 1. Reagents and conditions: a – EtOH, reflux, 5 h; b – NaOH, stirring, 18–24 h, rt; c – EtOH, reflux, NaOH, 8–12 h.

8–12 hours in 40 mL of 95 % ethanol. NaOH (10 mmol). The precipitated product was filtered, washed, and recrystallized from ethanol to furnish compounds **3a–j**, as shown in Scheme 1. The raw product is subjected to flash column chromatography (*n*-hexane/ethyl acetate, 8:2) for further purification.

Cells and biological assays

Cell culture. – RAW264.7 macrophage cells (ATCC, USA) were cultivated in Dulbecco's modified Eagle's medium (DMEM) supplemented with 10 % fetal calf serum (FCS), 2 mmol L^{-1} GlutaMax supplement (Thermo Fisher Scientific, USA) and 1 % (*V*/*V*) penicillin-streptomycin. The cells were maintained at 37 °C and 5 % CO_2. MCF-12A cells were maintained at 37 °C in a cell incubator, with a humid atmosphere with 5 % CO_2. Unless specified otherwise, the cells were cultured in T-flasks, containing DMEM, supplemented with phenol red, 10 % fetal bovine serum (FBS, Hyclone, USA), 25 mmol L^{-1} *N*-2-hydroxyethylpiperazine-*N*'-2-ethanesulfonic acid, 2 mmol L^{-1} L-glutamine and 1 % antibiotic–antimycotic mixture (Lonza, Belgium).

In vitro *NF-κB inhibitory activity*. – The inhibitory effect of the synthesized compounds on NF-κB transcription inhibitory activity was determined in RAW264.7 cells using a dual-luciferase reporter assay system (Promega, USA) as reported previously (15, 16).

MTT assay. – The effect of compound **3h** on the viability of MCF-12A cells (normal epithelial cells) was investigated using MTT assay as per the previously reported procedure (19).

Pharmacological activity

Animals. – The Sprague-Dawley (SD) rats (male, 7–9 weeks old, weighing 210–260 g) were obtained from the animal house of Henan Province Hospital of TCM, Zhengzhou, China, and all experiments were approved by the ethics committee of the same institution. The rats were housed in a suitable hygienic laboratory environment with an alternate light/dark cycle of 12 h each day and provided with standard food and water *ad libitum*.

Establishment of sepsis model. – The present study used the cecal ligation puncture (CLP) method to provoke sepsis in the SD rats. It is the most widely used method for creating sepsis in an animal model where the cecum of the animals is perforated using the needle. This perforation releases fecal material into the peritoneal cavity to generate an intense immune response induced by poly-microbial infection. This model fulfills the human condition that is clinically relevant. Briefly, the midline laparotomy was executed on the experimental animals after anesthetizing by mixing xylazine and ketamine hydrochloride at 10 and 100 mg kg^{-1}, resp. A 2-cm incision was made to the abdominal wall, and the cecum was exposed and ligated 0.5 cm from the tip with a 4–0 silk suture. A 22-gauge needle was used to punctured the cecum twice to the distal cecum, extruding a small amount of fecal contents.

The cecum was replaced into the abdominal cavity, and the exposed abdominal wall was closed in two layers with a running 4–0 silk suture. Neither ligation nor perforation was performed in the sham-treated group.

Experimental design. – The rats were divided into five groups (n = 6): group 1 – sham group, group 2 – cecal ligation and puncture (CLP), group 3 – CLP + compound **3h** (5 mg kg^{-1}), group 4 – CLP + compound **3h** (10 mg kg^{-1}), and group 5 – CLP + Dex (dexamethasone) in the dose of 5 mg kg^{-1}. The sham and the CLP groups were administered with normal saline (150 μL) 1 h before the operation *via* the *i.p.* route.

The rats were given compound **3h** in the dose of 5 or 10 mg kg^{-1} *i.p.* daily for 3 days before CLP surgery and on the 4th day 1 h before CLP. The rats in each group were anesthetized and were sacrificed 24 h after the CLP operation. The bronchoalveolar lavage (BAL) fluid from the left lung of rats was collected using 0.8 mL of normal saline. The withdrawn fluid was centrifuged at 15,000×*g*, and the supernatant was frozen and stored at –80 °C for further use. The blood collected *via* the orbital sinus was used for further biochemical analysis.

Histopathological assessment. – The lung tissues were immediately fixed in 4 % paraformaldehyde for at least 48 h just at room temperature, dehydrated by grading ethanol, and embedded in paraffin. Subsequently, the tissue specimens were cut into 5-μm slices, placed on glass slides, deparaffinized with xylene, hydrated with grading ethanol, and stained with the hematoxylin-eosin (H&E) solution. For examination, a typical laboratory light microscope with a magnification of 100× for use in pathology and a camera (Olympus DP71, Olympus Optical Co. Ltd, Japan) were used.

Determination of lung wet/dry mass ratio. – After removal from the experimental subjects, the excised rat lungs were weighed and then dried at 80 °C for 72 h until they gained a constant mass. The ratio of the wet lung to the dry lung mass was calculated.

Total protein and cell count of BALF. – The bronchoalveolar lavage fluid (BALF) was collected by washing the airways of rats thrice with saline, and the resulting solution was centrifuged for 10 min at 4 °C. The resulting supernatant was subjected to protein analysis using the bicinchoninic acid (BCA) protein assay kit. The cell pellets were re-suspended and stained with a Wright-Giemsa solution and leukocyte was determined using a hemocytometer.

Estimation of oxidative enzymes in the lung tissues. – In lung homogenate of experimental animals, activities of myeloperoxidase (MPO), superoxide dismutase (SOD), levels of malondialdehyde (MDA) and glutathione (GSH) were measured using commercial kits (Jiancheng Bioengineering Institute, China) as per the manufacturer's instructions.

Analysis of serum cytokines. – The levels of tumor necrosis factor (TNF)-α, interleukin (IL)-1β, and IL-6 in serum after separating from the blood were determined by ELISA assay using commercial kits (USCN Life Science Inc, China) as per the manufacturer's instructions.

Analysis of NF-κB using Western blot. – The isolated proteins from the lung tissues were separated by 10 % SDS-PAGE for 50 min and transferred to the polyvinylidene fluoride (PVDF) membrane. The membrane was blocked with 5 % non-fat milk in Tris-buffered saline with 0.1 % Tween 20 for 1 h at 4 °C and then incubated with anti-mouse NF-κB and GAPDH antibodies at 4 °C overnight. The membrane was further incubated with anti-

mouse IgG HRP-conjugated secondary antibodies. Corresponding protein expression was recorded with an ECL detection kit as per the previously reported procedure (20, 21).

Annexin V/PI assay. – After isolating lung alveolar macrophage cells from the BALF, the cells were seeded into 6-well plates at a density of 5×10^4 cells per well, cultured overnight, and treated with **3h** in Dulbecco's modified eagle medium (DMEM) for 24 hours. The supernatants containing cells trypsinized by non-EDTA trypsin (Gibco, USA) were collected. The cells were then centrifuged, stained with Annexin V-FITC and propidium iodide (PI; BioVision, USA), and analyzed with a flow cytometer (BD FACS Canto™, BD Biosciences, USA).

Statistical analysis

Results are shown as mean ± standard error of the mean (SEM) using the SPSS 19.0 (IBM, USA). The difference between groups was analyzed using ANOVA followed by the Bonferroni *post hoc* test.

RESULTS AND DISCUSSION

Chemistry

The synthesis of title compounds has been performed in a two-step procedure and depicted in Scheme 1. The first step corresponds to the synthesis of 8-(methylamino) imidazo[1,2-*a*]pyrazine-2-carbohydrazide (**1**) using ethyl 8-(methylamino) imidazo[1,2-*a*] pyrazine-2-carboxylate and hydrazine. The second step shows the synthesis of various chalcone derivatives **2a-j** *via* a reaction between 4-methoxybenzaldehyde and phenyl-substituted acetophenones. The intermediate compounds **2a-j** were further refluxed with compound **1** in the presence of ethanol and base to afford target compounds **3a-j**. The compounds were purified by recrystallization and obtained in high yield (Table I).

Physicochemical and spectral data for intermediates and target compounds are given in Tables I and II. FT-IR peak of title compounds at 3345–3348 cm^{-1} was due to the secondary amine (N-H) group attached to imidazopyrazine moiety. Stretching vibration of the C-H group of aromatic phenyl ring linkage with pyrazole appeared at 3068–3094 cm^{-1}. Absorption bands at 2871–2879 cm^{-1} were caused by the stretching vibration of the phenyl ring's CH_3 group. Other peaks were obtained at 1708–1723 cm^{-1} as a result of the C=O group. Furthermore, a band at 1161–1169 cm^{-1} was assigned to the fluoro group attached to a phenyl ring. At 1214–1247 cm^{-1}, the stretching vibration of the phenyl ring C=C group appeared. Another peak appeared at 1539 cm^{-1} due to the presence of a NO_2 group connected to an aromatic ring, while the stretching vibration of the OH group linkage with the phenyl ring causes an absorption band at 3284 cm^{-1}.

Furthermore, the title compounds were confirmed by ^1H NMR spectra, which revealed a singlet peak attributable to O-H groups attached to phenyl rings at 10.23 ppm. The C-H proton of the aromatic phenyl ring connected with the pyrazole ring showed doublets at 7.14–7.21 ppm. The aromatic proton doublets were detected at 8.68–8.61 ppm due to the imidazopyrazine ring. The C-H group proton was detected as doublets at 7.98–8.05 ppm due to the pyrazole ring. Because of the CH_3 group linkage with the phenyl ring, the

Table I. Physicochemical characteristics of the synthesized compounds

Compd.	Chemical name	Molecular formula	M_r	Yield (%)	M. p. (°C)	CHN analysis (calcd./found)	R_f value
1	8-(methylamino)imidazo[1,2-*a*]pyrazine-2-carbohydrazide	$C_8H_{10}N_6O$	206.21	87	196–198	C, 46.60; H, 4.89; N, 40.76 C, 46.55; H, 4.90; N, 40.75	0.69
2a	3-(4-methoxyphenyl)-1-(4-((trifluoromethyl)thio)phenyl) prop-2-en-1-one	$C_{17}H_{13}F_3O_2S$	338.34	78	203–204	C, 60.35; H, 3.87 C, 60.42; H, 8.92	0.74
2b	3-(4-methoxyphenyl)-1-(4-(methylsulfonyl)phenyl) prop-2-en-1-one	$C_{17}H_{16}O_4S$	316.37	84	211–212	C, 64.54; H, 5.10 C, 64.61; H, 5.08	0.69
2c	4-(3-(4-methoxyphenyl)acryloyl)benzenesulfonamide	$C_{16}H_{15}NO_4S$	317.36	76	215–216	C, 60.55; H, 4.76; N, 4.41 C, 60.53; H, 4.70; N, 4.43	0.71
2d	3-(4-methoxyphenyl)-1-(4-(methylthio)phenyl)prop--2-en-1-one	$C_{17}H_{16}O_2S$	284.37	85	184–185	C, 71.80; H, 5.67 C, 71.84; H, 5.62	0.78
2e	3-(4-methoxyphenyl)-1-(4-tosylphenyl)prop-2-en-1-one	$C_{23}H_{20}O_4S$	392.47	72	246–248	C, 70.39; H, 5.14 C, 70.42; H, 5.13	0.83
2f	3-(4-methoxyphenyl)-1-(4-((4-nitrophenyl)sulfonyl)phenyl) prop-2-en-1-one	$C_{22}H_{17}NO_6S$	423.44	78	258–259	C, 62.40; H, 4.05; N, 3.31 C, 62.43; H, 4.07; N, 3.36	0.54
2g	1-(4-((4-chlorophenyl)sulfonyl)phenyl)-3-(4-methoxyphenyl)prop-2-en-1-one	$C_{22}H_{17}ClO_4S$	412.88	80	252–253	C, 64.00; H, 4.15 C, 64.05; H, 4.16	0.79
2h	1-(4-((4-hydroxyphenyl)sulfonyl)phenyl)-3-(4-methoxyphenyl)-prop-2-en-1-one	$C_{22}H_{18}O_5S$	394.44	87	227–228	C, 66.99; H, 4.60 C, 67.03; H, 4.64	0.72
2i	3-(4-methoxyphenyl)-1-(4-((4-methoxyphenyl)sulfonyl) phenyl)-prop-2-en-1-one	$C_{23}H_{20}O_5S$	408.47	81	243–244	C, 67.63; H, 4.94 C, 67.66; H, 4.92	0.89
2j	1-(4-((4-fluorophenyl)sulfonyl)phenyl)-3-(4-methoxyphenyl)prop-2-en-1-one	$C_{22}H_{17}FO_4S$	396.43	76	261–262	C, 66.55; H, 4.32 C, 66.59; H, 4.30	0.81

3a	(5-(4-methoxyphenyl)-4-(4-((trifluoromethyl)thio) phenyl)-4,5-dihydro-1*H*-pyrazol-1-yl)(8-(methylamino) imidazo[1,2-*a*]pyrazin-2-yl)methanone	$C_{25}H_{21}F_3N_6O_2S$	526.54	83	267–268	C, 57.03; H, 4.02; N, 15.96 C, 57.06; H, 4.07; N, 15.92	0.72
3b	(5-(4-methoxyphenyl)-4-(4-(methylsulfonyl)phenyl)-4,5-dihydro-1*H*-pyrazol-1-yl)(8-(methylamino)imidazo[1,2-*a*] pyrazin-2-yl)-methanone	$C_{25}H_{24}N_6O_4S$	504.57	72	258–259	C, 59.51; H, 4.79; N, 16.66 C, 59.56; H, 4.78; N, 16.65	0.56
3c	4-(5-(4-methoxyphenyl)-1-(8-(methylamino)imidazo[1,2-*a*] pyrazine-2-carbonyl)-4,5-dihydro-1*H*-pyrazol-4-yl)-benzenesulfonamide	$C_{24}H_{23}N_7O_4S$	505.55	79	269–270	C, 57.02; H, 4.59; N, 19.39 C, 57.04; H, 4.63; N, 19.45	0.67
3d	(5-(4-methoxyphenyl)-4-(4-(methylthio)phenyl)-4,5-dihydro-1*H*-pyrazol-1-yl)(8-(methylamino)imidazo[1,2-*a*] pyrazin-2-yl)-methanone	$C_{25}H_{24}N_6O_2S$	472.57	73	282–283	C, 63.54; H, 5.12; N, 17.78 C, 63.57; H, 5.08; N, 17.79	0.49
3e	(5-(4-methoxyphenyl)-4-(4-tosylphenyl)-4,5-dihydro-1*H*-pyrazol-1-yl)(8-(methylamino)imidazo[1,2-*a*]pyrazin-2-yl) methanone	$C_{31}H_{28}N_6O_4S$	580.66	82	294–295	C, 64.12; H, 4.86; N, 14.47 C, 64.08; H, 4.85; N, 14.52	0.68
3f	(5-(4-methoxyphenyl)-4-(4-((4-nitrophenyl)sulfonyl) phenyl)-4,5-dihydro-1*H*-pyrazol-1-yl)(8-(methylamino) imidazo[1,2-*a*]pyrazin-2-yl)methanone	$C_{30}H_{25}N_7O_6S$	611.63	69	301–302	C, 58.91; H, 4.12; N, 16.03 C, 58.87; H, 4.16; N, 16.05	0.62
3g	(4-(4-((4-chlorophenyl)sulfonyl)phenyl)-5-(4-methoxyphenyl)-4,5-dihydro-1*H*-pyrazol-1-yl)(8-(methylamino)imidazo[1,2-*a*]pyrazin-2-yl)methanone	$C_{30}H_{25}ClN_6O_4S$	601.08	76	298–299	C, 59.95; H, 4.19; N, 13.98 C, 59.99; H, 4.17; N, 13.97	0.73
3h	(4-(4-((4-hydroxyphenyl)sulfonyl)phenyl)-5-(4-methoxyphenyl)-4,5-dihydro-1*H*-pyrazol-1-yl)(8-(methylamino)imidazo[1,2-a] pyrazin-2-yl)methanone	$C_{30}H_{26}N_6O_5S$	582.64	83	291–292	C, 61.84; H, 4.50; N, 14.42 C, 61.86; H, 4.47; N, 14.40	0.79
3i	(5-(4-methoxyphenyl)-4-(4-((4-methoxyphenyl)sulfonyl) phenyl)-4,5-dihydro-1*H*-pyrazol-1-yl)(8-(methylamino) imidazo[1,2-*a*] pyrazin-2-yl)methanone	$C_{31}H_{28}N_6O_5S$	596.66	87	304–305	C, 62.40; H, 4.73; N, 14.09 C, 62.45; H, 4.69; N, 14.07	0.84
3j	(4-(4-((4-fluorophenyl)sulfonyl)phenyl)-5-(4-methoxyphenyl)-4,5-dihydro-1*H*-pyrazol-1-yl)(8-(methylamino)imidazo[1,2-*a*]pyrazin-2-yl)methanone	$C_{30}H_{25}FN_6O_4S$	584.63	82	289–290	C, 61.63; H, 4.31; N, 14.38 C, 61.67; H, 4.29; N, 14.37	0.71

Table II. Synthesized compounds' spectral data

Compd.	FTIR (KBr, ν_{max}, cm^{-1})	^1H NMR (400M Hz, DMSO-d_6, TMS) (δ, ppm)	^{13}C NMR (100 MHz, DMSO-d_6) (δ, ppm)	Mass: $(M+H)^+$
1	3348 (N-H), 3081 (aromatic C-H), 2879 (CH_3), 1719 (C=O), 1659 (CO-NH), 1548 (C=N), 1469 (CH_3 bending), 1239 (C-N), 1214 (C=C), 887	9.59 (1H, s, NH-imidazo pyrazine), 8.67 (d, 1H, *J* = 7.34 Hz, imidazo pyrazine-H), 8.53 (d, 1H, *J* = 1.97 Hz, imidazo pyrazine-H), 7.25 (d, 1H, *J* = 1.82 Hz, imidazo pyrazine-H), 4.59 (s, 2H, NH_2), 3.93 (1H, s, NH × 1), 2.57 (3H, s, imidazo pyrazine -CH_3)	161.5, 149.7, 132.4, 127.8, 122.5, 117.1, 108.8, 27.3	207.23
2a	3068 (aromatic C-H), 2834 (OCH_3), 1708 (C=O), 1218 (C=C), 1168 (C-F), 887, 738 (C-S)	8.03 (d, 2H, *J* =1.49 Hz, Ar-H), 7.83 (d, 2H, *J* = 1.82 Hz, Ar-H), 7.65 (d, 1H, *J* = 15.28 Hz, aliphatic-H), 7.49 (d, 2H, *J* = 1.73 Hz, Ar-H), 7.20 (d, 2H, *J* = 1.23 Hz, Ar-H), 6.72 (d, 1H, *J* = 15.21 Hz, aliphatic-H), 3.72 (s, 3H, OCH_3)	189.8, 159.7, 145.2, 142.4, 137.8, 134.5, 130.5, 128.9, 127.7, 127.2, 121.4, 114.3, 55.9	339.37
2b	3078 (aromatic C-H), 2842 (OCH_3), 1716 (C=O), 1223 (C=C), 1156 (SO_2), 894, 743 (C-S)	8.01 (d, 2H, *J* = 1.53 Hz, Ar-H), 7.81 (d, 2H, *J* = 1.93 Hz, Ar-H), 7.62 (d, 1H, *J* = 15.59 Hz, aliphatic-H), 7.50 (d, 2H, *J* = 1.78 Hz, Ar-H), 7.25 (d, 2H, *J* = 1.29 Hz, Ar-H), 6.67 (d, 1H, *J* = 15.48 Hz, aliphatic-H), 3.79 (s, 3H, OCH_3), 3.07 (s, 3H, CH_3)	189.8, 159.7, 146.9, 145.2, 142.8, 130.7, 130.1, 128.9, 127.5, 121.4, 114.3, 55.8, 47.9	317.37
2c	3345 (N-H), 3072 (aromatic C-H), 2848 (OCH_3), 1709 (C=O), 1229 (C=C), 1151 (SO_2), 897, 741 (C-S)	10.32 (s, 2H, NH_2), 7.97 (d, 2H, *J* = 1.49 Hz, Ar-H), 7.72 (d, 2H, *J* = 2.21 Hz, Ar-H), 7.67 (d, 1H, *J* = 15.42 Hz, aliphatic-H), 7.45 (d, 2H, *J* = 1.70 Hz, Ar-H), 7.18 (d, 2H, *J* = 1.21 Hz, Ar-H), 6.69 (d, 1H, *J* = 15.57 Hz, aliphatic-H), 3.72 (s, 3H, OCH_3)	190.1, 160.2, 149.8, 145.3, 141.2, 130.9, 130.1, 127.9, 127.2, 121.5, 114.2, 55.8	318.38
2d	3084 (aromatic C-H), 2842 (OCH_3), 1721 (C=O), 1223 (C=C), 891, 748 (C-S)	7.65 (d, 2H, *J* = 1.28 Hz, Ar-H), 7.58 (d, 2H, *J* = 1.79 Hz, Ar-H), 7.42 (d, 1H, *J* = 15.61 Hz, aliphatic-H), 7.49 (d, 2H, *J* = 1.76 Hz, Ar-H), 7.23 (d, 2H, *J* = 1.25 Hz, Ar-H), 6.61 (d, 1H, *J* = 15.52 Hz, aliphatic-H), 3.78 (s, 3H, OCH_3), 2.56 (s, 3H, SCH_3)	189.4, 160.1, 145.6, 145.1, 134.7, 130.5, 128.8, 127.5, 127.3, 121.2, 114.6, 55.9, 14.9	285.37
2e	3092 (aromatic C-H), 2871 (CH_3), 2849 (OCH_3), 1714 (C=O), 1482 (CH_3 bending), 1229 (C=C), 1158 (SO_2), 897, 743 (C-S)	8.05 (d, 2H, *J* = 1.49 Hz, Ar-H), 7.75 (d, 2H, *J* = 1.72 Hz, Ar-H), 7.65 (d, 1H, *J* = 15.51 Hz, aliphatic-H), 7.61 (d, 2H, *J* = 1.53 Hz, Ar-H), 7.51 (d, 2H, *J* = 1.72 Hz, Ar-H), 7.32 (d, 2H, *J* = 1.91 Hz, Ar-H), 7.19 (d, 2H, *J* = 1.21 Hz, Ar-H), 6.73 (d, 1H, *J* = 15.42 Hz, aliphatic-H), 3.81 (s, 3H, OCH_3), 2.32 (s, 3H, CH_3)	190.1, 159.9, 147.3, 145.2, 142.8, 139.5, 138.6, 130.8, 130.1, 129.9, 128.9, 128.2, 127.7, 121.3, 114.2, 55.8, 21.5	393.47

2f	3098 (aromatic C-H), 2853 (OCH_3), 1709 (C=O), 1539 (NO_2), 1234 (C=C), 1163 (SO_2), 883, 748 (C-S)	8.10 (d, 2H, *J* = 2.11 Hz, Ar-H), 8.03 (d, 2H, *J* = 2.27 Hz, Ar-H), 7.99 (d, 2H, *J* = 1.49 Hz, Ar-H), 7.76 (d, 2H, *J* = 1.73 Hz, Ar-H),7.67 (d, 1H, *J* = 15.59 Hz, aliphatic-H), 7.49 (d, 2H, *J* = 1.71 Hz, Ar-H), 7.21 (d, 2H, *J* = 1.23 Hz, Ar-H), 6.75 (d, 1H, *J* = 15.46 Hz, aliphatic-H), 3.79 (s, 3H, OCH_3)	189.9, 159.7, 152.8, 147.6, 147.2, 145.1, 142.7, 130.9, 130.2, 129.3, 128.8, 127.5, 124.9, 121.3, 114.2, 55.7	424.44
2g	3087 (aromatic C-H), 2859 (OCH_3), 1712 (C=O), 1238 (C=C), 1162 (SO_2), 887, 768 (C-Cl), 742 (C-S)	7.98 (d, 2H, *J* = 1.49 Hz, Ar-H), 7.73 (d, 2H, *J* = 1.78 Hz, Ar-H), 7.67 (d, 2H, *J* = 1.56 Hz, Ar-H), 7.62 (d, 1H, *J* = 15.52 Hz, aliphatic-H), 7.59 (d, 2H, *J* = 1.93 Hz, Ar-H), 7.53 (d, 2H, *J* = 1.68 Hz, Ar-H), 7.18 (d, 2H, *J* = 1.28 Hz, Ar-H), 6.70 (d, 1H, *J* = 15.41 Hz, aliphatic-H), 3.75 (s, 3H, OCH_3)	189.2, 159.4, 147.8, 145.2, 142.9, 139.5, 139.1, 130.9, 130.3, 129.8, 129.7, 128.8, 127.4, 114.3, 121.2, 55.3	413.90
2h	3284 (O-H), 3083 (aromatic C-H), 2868 (OCH_3), 1719 (C=O), 1243 (C=C), 1168 (SO_2), 882, 747 (C-S)	9.23 (s, 1H, Ar-OH), 8.01 (d, 2H, *J* = 1.56 Hz, Ar-H), 7.71 (d, 2H, *J* = 1.74 Hz, Ar-H), 7.66 (d, 1H, *J* = 15.49 Hz, aliphatic-H), 7.60 (d, 2H, *J* = 1.52 Hz, Ar-H), 7.47 (d, 2H, *J* = 1.73 Hz, Ar-H), 7.23 (d, 2H, *J* = 1.21 Hz, Ar-H), 7.12 (d, 2H, *J* = 1.29 Hz, Ar-H), 6.65 (d, 1H, *J* = 15.52 Hz, aliphatic-H), 3.72 (s, 3H, OCH_3)	190.1, 159.9, 163.5, 147.5, 145.1, 142.8, 134.0, 130.9, 130.2, 130.6, 129.8, 128.9, 127.5, 121.4, 114.3, 55.9	395.46
2i	3087 (aromatic C-H), 2862 (OCH_3), 1723 (C=O), 1247 (C=C), 1165 (SO_2), 887, 752 (C-S)	8.03 (d, 2H, *J* = 1.52 Hz, Ar-H), 7.74 (d, 2H, *J* = 1.79 Hz, Ar-H), 7.63 (d, 1H, *J* = 15.59 Hz, aliphatic-H), 7.59 (d, 2H, *J* = 1.55 Hz, Ar-H), 7.51 (d, 2H, *J* = 1.75 Hz, Ar-H), 7.21 (d, 2H, *J* = 1.27 Hz, Ar-H), 6.97 (d, 2H, *J* = 1.46 Hz, Ar-H), 6.68 (d, 1H, *J* = 15.46 Hz, aliphatic-H), 3.79 (s, 3H, OCH_3), 3.85 (s, 3H, OCH_3)	189.9, 165.7, 159.9, 147.3, 145.1, 142.8, 133.8, 130.9, 130.1, 129.4, 128.9, 127.5, 115.5, 121.4, 55.9, 55.3, 114.4	409.48
2j	3094 (aromatic C-H), 2868 (OCH_3), 1715 (C=O), 1243 (C=C), 1187 (C-F), 1169 (SO_2), 888, 757 (C-S)	7.97 (d, 2H, *J* = 1.49 Hz, Ar-H), 7.91 (d, 2H, *J* = 1.56 Hz, Ar-H), 7.72 (d, 2H, *J* = 1.78 Hz, Ar-H), 7.68 (d, 1H, *J* = 15.49 Hz, aliphatic-H), 7.63 (d, 2H, *J* = 1.62 Hz, Ar-H),7.49 (d, 2H, *J* = 1.73 Hz, Ar-H), 7.23 (d, 2H, *J* = 1.25 Hz, Ar-H), 6.63 (d, 1H, *J* = 15.49 Hz, aliphatic-H), 3.83 (s, 3H, OCH_3)	190.2, 167.8, 160.2, 147.4, 145.1, 142.8, 137.1, 130.9, 130.2, 129.9, 128.8, 127.7, 121.5, 116.5, 114.3, 55.9	397.43
3a	3345 (N-H), 3072 (aromatic C-H), 2878 (CH_3), 2847 (OCH_3), 1719 (C=O), 1628 (C=N), 1234 (C-N), 1214 (C=C), 1175 (C-F), 892, 734 (C-S)	^{1}H NMR (400MHz, DMSO-d_6, TMS) δ ppm: 9.47 (1H, s, imidazo pyrazine-NH), 8.67 (d, 1H, *J* = 1.96 Hz, imidazo pyrazine-H), 8.60 (d, 1H, *J* = 0.54 Hz, imidazo pyrazine-H), 8.03 (d, 1H, *J* = 4.78 Hz, pyrazole-H), 7.54 (d, 2H, *J* = 1.36 Hz, Ar-H),7.26 (d, 1H, *J* = 0.51 Hz, imidazo pyrazine-H) 7.15 (d, 2H, *J* = 1.28 Hz, Ar-H), 6.75 (d, 2H, *J* = 1.52 Hz, Ar-H), 6.92 (d, 2H, *J* = 1.21 Hz, Ar-H), 5.60 (d, 1H, *J* = 8.06 Hz, pyrazole-H), 4.34 (d, 1H, *J* = 4.72 Hz, pyrazole-H), 3.74 (s, 3H, OCH_3), 2.60 (s, 3H, CH_3)	168.7, 158.7, 149.6, 149.0, 137.1, 136.8, 135.8, 133.7, 132.1, 128.7, 127.9, 127.5, 126.6, 122.5, 117.1, 114.1, 108.8, 58.5, 55.8, 43.9, 27.2	527.54

3b	3353 (N-H), 3078 (aromatic C-H), 2881 (CH_3), 2849 (OCH_3), 1712 (C=O), 1624 (C=N), 1237 (C-N), 1208 (C=C), 1173 (SO_2), 897, 738 (C-S)	9.56 (1H, s, imidazo pyrazine-NH), 8.64 (d, 1H, *J* = 1.92 Hz, imidazo pyrazine-H), 8.57 (d, 1H, *J* = 0.51 Hz, imidazo pyrazine-H), 8.07 (d, 1H, *J* = 4.72 Hz, pyrazole-H), 7.70 (d, 2H, *J* = 1.56 Hz, Ar-H), 7.61 (d, 2H, *J* = 1.53 Hz, Ar-H),7.29 (d, 1H, *J* = 0.54 Hz, imidazo pyrazine-H) 7.18 (d, 2H, *J* = 1.25 Hz, Ar-H), 6.87 (d, 2H, *J* = 1.24 Hz, Ar-H), 5.82 (d, 1H, *J* = 8.03 Hz, pyrazole-H), 4.47 (d, 1H, *J* = 4.79 Hz, pyrazole-H), 3.76 (s, 3H, OCH_3), 3.07 (s, 3H, CH_3), 2.62 (s, 3H, CH_3)	169.4, 159.7, 149.8, 149.3, 145.7, 138.4, 135.9, 132.1, 128.7, 128.5, 127.9, 126.9, 122.4, 117.2, 114.3, 108.9, 58.7, 55.9, 47.7, 43.7, 27.3	505.59
3c	3359 (N-H), 3072 (aromatic C-H), 2885 (CH_3), 2841 (OCH_3), 1719 (C=O), 1629 (C=N), 1232 (C-N), 1216 (C=C), 1185 (SO_2), 891, 743 (C-S)	9.59 (1H, s, imidazo pyrazine-NH), 8.68 (d, 1H, *J* = 1.96 Hz, imidazo pyrazine-H), 8.62 (d, 1H, *J* = 0.58 Hz, imidazo pyrazine-H), 8.13 (d, 1H, *J* = 4.81 Hz, pyrazole-H), 7.81 (d, 2H, *J* = 1.51 Hz, Ar-H), 7.79 (d, 2H, *J* = 1.50 Hz, Ar-H), 7.35 (s, 2H, SO_2NH_2), 7.24 (d, 1H, *J* = 0.59 Hz, imidazo pyrazine-H) 7.15 (d, 2H, *J* = 1.29 Hz, Ar-H), 6.92 (d, 2H, *J* = 1.27 Hz, Ar-H), 5.74 (d, 1H, *J* = 8.01 Hz, pyrazole-H), 4.52 (d, 1H, *J* = 4.73 Hz, pyrazole-H), 3.74 (s, 3H, OCH_3), 2.64 (s, 3H, CH_3)	168.2, 158.7, 149.5, 149.1, 143.9, 140.8, 135.9, 132.3, 128.5, 128.1, 127.8, 126.7, 122.8, 117.2, 114.3, 108.7, 58.5, 55.9, 43.8, 27.4	506.55
3d	3368 (N-H), 3071 (aromatic C-H), 2889 (CH3), 2846 (OCH_3), 1713 (C=O), 1632 (C=N), 1237 (C-N), 1219 (C=C), 1187 (SO2), 893, 745 (C-S)	9.53 (1H, s, imidazo pyrazine-NH), 8.63 (d, 1H, *J* = 1.98 Hz, imidazo pyrazine-H), 8.59 (d, 1H, *J* = 0.53 Hz, imidazo pyrazine-H), 8.03 (d, 1H, *J* = 4.76 Hz, pyrazole-H), 7.28 (d, 1H, *J* = 0.51 Hz, imidazo pyrazine-H) 7.21 (d, 2H, *J* = 1.35 Hz, Ar-H), 7.17 (d, 2H, *J* = 1.32 Hz, Ar-H), 6.89 (d, 2H, *J* = 1.24 Hz, Ar-H), 6.86 (d, 2H, *J* = 1.21 Hz, Ar-H), 5.59 (d, 1H, *J* = 8.07 Hz, pyrazole-H), 4.35 (d, 1H, *J* = 4.78 Hz, pyrazole-H), 3.78 (s, 3H, OCH3), 2.59 (s, 3H, CH3), 2.45 (s, 3H, SCH_3)	169.3, 158.9, 150.2, 149.2, 139.8, 137.2, 135.9, 132.5, 128.9, 127.8, 127.7, 126.8, 122.4, 117.1, 108.7, 114.2, 58.7, 55.9, 27.3, 14.9	473.57
3e	3375 (N-H), 3077 (aromatic C-H), 2894 (CH3), 2856 (OCH3), 1723 (C=O), 1637 (C=N), 1231 (C-N), 1216 (C=C), 1189 (SO_2), 891, 752 (C-S)	9.47 (1H, s, imidazo pyrazine-NH), 8.69 (d, 1H, *J* = 1.92 Hz, imidazo pyrazine-H), 8.60 (d, 1H, *J* = 0.55 Hz, imidazo pyrazine-H), 8.01 (d, 1H, *J* = 4.79 Hz, pyrazole-H), 7.69 (d, 2H, *J* = 1.55 Hz, Ar-H), 7.65 (d, 2H, *J* = 1.53 Hz, Ar-H), 7.60 (d, 2H, *J* = 1.51 Hz, Ar-H), 7.32 (d, 2H, *J* = 1.92 Hz, Ar-H), 7.24 (d, 1H, *J* = 0.53 Hz, imidazo pyrazine-H), 7.19 (d, 2H, *J* = 1.35 Hz, Ar-H), 6.87 (d, 2H, *J* = 1.21 Hz, Ar-H), 5.76 (d, 1H, *J* = 8.03 Hz, pyrazole-H), 4.48 (d, 1H, *J* = 4.68 Hz, pyrazole-H), 3.75 (s, 3H, OCH3), 2.61 (s, 3H, CH3), 2.32 (s, 3H, CH_3)	168.5, 159.9, 149.5, 149.1, 145.7, 139.4, 138.7, 138.5, 135.9, 132.1, 130.1, 128.9, 128.2, 128.1, 127.8, 126.6, 122.5, 117.1, 108.7, 114.2, 58.5, 55.9, 43.8, 27.6, 21.5	581.65

3f	3386 (N-H), 3079 (aromatic C-H), 2883 (CH_3), 2859 (OCH_3), 1718 (C=O), 1641 (C=N), 1548 (NO_2), 1234 (C-N), 1214 (C=C), 1192 (SO_2), 885, 757 (C-S)	9.38 (1H, s, imidazo pyrazine-NH), 8.71 (d, 1H, *J* = 1.96 Hz, imidazo pyrazine-H), 8.56 (d, 1H, *J* = 0.59 Hz, imidazo pyrazine-H), 8.12 (d, 2H, *J* = 2.10 Hz, Ar-H), 8.05 (d, 1H, *J* = 4.74 Hz, pyrazole-H), 8.02 (d, 2H, *J* = 2.27 Hz, Ar-H), 7.67 (d, 2H, *J* = 1.55 Hz, Ar-H), 7.65 (d, 2H, *J* = 1.52 Hz, Ar-H), 7.28 (d, 1H, *J* = 0.48 Hz, imidazo pyrazine-H), 7.21 (d, 2H, *J* = 1.37 Hz, Ar-H), 6.91 (d, 2H, *J* = 1.23 Hz, Ar-H), 5.81 (d, 1H, *J* = 8.07 Hz, pyrazole-H), 4.45 (d, 1H, *J* = 4.72 Hz, pyrazole-H), 3.72 (s, 3H, OCH_3), 2.66 (s, 3H, CH_3)	168.9, 159.2, 152.8, 149.5, 149.1, 147.6, 145.8, 138.9, 135.9, 132.1, 129.2, 128.7, 128.2, 127.9, 126.8, 124.9, 122.5, 117.1, 114.3, 108.8, 58.5, 55.8, 43.9, 27.3	612.65
3g	3381 (N-H), 3083 (aromatic C-H), 2885 (CH_3), 2862 (OCH_3), 1715 (C=O), 1645 (C=N), 1237 (C-N), 1215 (C=C), 1197 (SO_2), 881, 762 (C-Cl), 754 (C-S)	9.45 (1H, s, imidazo pyrazine-NH), 8.63 (d, 1H, *J* = 1.92 Hz, imidazo pyrazine-H), 8.60 (d, 1H, *J* = 0.54 Hz, imidazo pyrazine-H), 8.07 (d, 1H, *J* = 4.79 Hz, pyrazole-H), 7.69 (d, 2H, *J* = 1.54 Hz, Ar-H), 7.67 (d, 2H, *J* = 1.58 Hz, Ar-H), 7.63 (d, 2H, *J* = 1.56 Hz, Ar-H), 7.61 (d, 2H, *J* = 1.93 Hz, Ar-H), 7.23 (d, 1H, *J* = 0.52 Hz, imidazo pyrazine-H), 7.19 (d, 2H, *J* = 1.35 Hz, Ar-H), 6.87 (d, 2H, *J* = 1.24 Hz, Ar-H), 5.73 (d, 1H, *J* = 8.02 Hz, pyrazole-H), 4.42 (d, 1H, *J* = 4.68 Hz, pyrazole-H), 3.76 (s, 3H, OCH_3), 2.62 (s, 3H, CH_3)	167.9, 159.3, 149.8, 149.0, 145.2, 139.7, 139.2, 138.5, 135,9, 132.2, 129.8, 129.3, 128.9, 128.1, 127.8, 126.8, 122.5, 117.2, 114.3, 108.6, 58.7, 55.9, 43.9, 27.3	602.10
3h	3374 (N-H), 3292 (O-H), 3085 (aromatic C-H), 2889 (CH_3), 2865 (OCH_3), 1719 (C=O), 1642 (C=N), 1231 (C-N), 1213 (C=C), 1192 (SO_2), 885, 762 (C-S)	10.23 (s, 1H, Ar-OH), 9.42 (1H, s, imidazo pyrazine-NH), 8.68 (d, 1H, *J* = 1.95 Hz, imidazo pyrazine-H), 8.57 (d, 1H, *J* = 0.51 Hz, imidazo pyrazine-H), 8.03 (d, 1H, *J* = 4.72 Hz, pyrazole-H), 7.63 (d, 2H, *J* = 1.56 Hz, Ar-H), 7.58 (d, 2H, *J* = 1.57 Hz, Ar-H), 7.61 (d, 2H, *J* = 1.54 Hz, Ar-H), 7.28 (d, 1H, *J* = 0.48 Hz, imidazo pyrazine-H), 7.21 (d, 2H, *J* = 1.32 Hz, Ar-H), 7.14 (d, 2H, *J* = 1.29 Hz, Ar-H), 6.92 (d, 2H, *J* = 1.18 Hz, Ar-H), 5.78 (d, 1H, *J* = 8.07 Hz, pyrazole-H), 4.45 (d, 1H, *J* = 4.72 Hz, pyrazole-H), 3.79 (s, 3H, OCH_3), 2.65 (s, 3H, CH_3)	168.5, 163.6, 158.2, 149.2, 149.1, 145.9, 138.8, 135.9, 134.1, 132.1, 130.7, 129.8, 128.7, 128.1, 127.8, 126.2, 122.9, 117.3, 114.2, 108.9, 58.7, 55.2, 43.8, 27.4	583.64
3i	3379 (N-H), 3092 (aromatic C-H), 2881 (CH_3), 2875 (OCH_3), 1721 (C=O), 1649 (C=N), 1229 (C-N), 1218 (C=C), 1197 (SO_2), 881, 764 (C-S)	9.47 (1H, s, imidazo pyrazine-NH), 8.73 (d, 1H, *J* = 1.99 Hz, imidazo pyrazine-H), 8.62 (d, 1H, *J* = 0.54 Hz, imidazo pyrazine-H), 8.06 (d, 1H, *J* = 4.78 Hz, pyrazole-H), 7.67 (d, 2H, *J* = 1.53 Hz, Ar-H), 7.61 (d, 2H, *J* = 1.52 Hz, Ar-H), 7.59 (d, 2H, *J* = 1.51 Hz, Ar-H), 7.22 (d, 1H, *J* = 0.57 Hz, imidazo pyrazine-H), 7.19 (d, 2H, *J* = 1.36 Hz, Ar-H), 6.98 (d, 2H, *J* = 1.48 Hz, Ar-H), 6.85 (d, 2H, *J* = 1.23 Hz, Ar-H), 5.72 (d, 1H, *J* = 8.02 Hz, pyrazole-H), 4.44 (d, 1H, *J* = 4.70 Hz, pyrazole-H), 3.86 (s, 3H, OCH_3), 3.75 (s, 3H, OCH_3), 2.59 (s, 3H, CH_3)	169.2, 165.6, 158.7, 149.5, 149.3, 145.8, 138.8, 135.9, 133.7, 132.1, 129.5, 128.5, 128.3, 127.7, 126.6, 122.5, 117.2, 115.4, 114.2, 108.7, 58.6, 55.9, 55.4, 43.3, 27.4	597.67

3j	3373 (N-H), 3097 (aromatic C-H), 2884 (CH_3), 2878 (OCH_3), 1718 (C=O), 1652 (C=N), 1221 (C-N), 1217 (C=C), 1192 (SO_2), 1183 (C-F), 885, 767 (C-S)	9.52 (1H, s, imidazo pyrazine-NH), 8.71 (d, 1H, *J* = 1.95 Hz, imidazo pyrazine-H), 8.59 (d, 1H, *J* = 0.51 Hz, imidazo pyrazine-H), 8.03 (d, 1H, *J* = 4.71 Hz, pyrazole-H), 7.91 (d, 2H, *J* = 1.57 Hz, Ar-H), 7.67 (d, 2H, *J* = 1.56 Hz, Ar-H), 7.62 (d, 2H, *J* = 1.47 Hz, Ar-H), 7.59 (d, 2H, *J* = 1.65 Hz, Ar-H), 7.28 (d, 1H, *J* = 0.50 Hz, imidazo pyrazine-H), 7.14 (d, 2H, *J* = 1.32 Hz, Ar-H), 6.91 (d, 2H, *J* = 1.19 Hz, Ar-H), 5.81 (d, 1H, *J* = 8.07 Hz, pyrazole-H), 4.49 (d, 1H, *J* = 4.73 Hz, pyrazole-H), 3.89 (s, 3H, OCH_3), 2.62 (s, 3H, CH_3)	169.1, 167.5, 158.8, 149.5, 149.2, 145.7, 138.7, 137.0, 135.9, 132.0, 129.9, 128.9, 128.1, 127.9, 126.8, 122.5, 114.1, 117.1, 116.7, 108.7, 58.7, 55.9, 43.9, 27.3	585.63

aliphatic proton appeared as a singlet at 3.79–3.89 ppm. Furthermore, an OCH_3 group showed a singlet peak at 2.61–2.68 ppm.

In ^{13}C NMR spectra, the carbon atom of the imidazopyrazine ring appeared at 108.6–149.4 ppm. The phenyl ring's aromatic carbon atoms were apparent at 114.1–167.9 ppm. Moreover, the pyrazole ring's aromatic carbon atoms that are linked to the phenyl ring were observed at 43.9–149.1 ppm. The peak at 165.9–167.4 ppm corresponds to the carbon atom of the ketone group linked with the phenyl ring.

Both elemental analysis and mass spectral analysis were found in accordance with the proposed chemical structures and mass of the final hybrid derivatives **3a–j**.

NF-κB inhibitory activity and structure-activity relationship (SAR)

The effects of target compounds were investigated on the NF-κB transcriptional activity in LPS-stimulated RAW264.7 cells. Table III shows that compound **3a** containing trifluoromethyl sulfane showed the least inhibitory activity with IC_{50} of 94.02 μmol L^{-1}. The inhibitory activity was significantly improved by the insertion of methyl sulphonyl in the case of compound **3b** (IC_{50} = 2.67 μmol L^{-1}). Marked drop in activity was reported for compounds **3c** (IC_{50} = 7.34 μmol L^{-1}), **3d** (IC_{50} = 15.02 μmol L^{-1}), **3e** (IC_{50} = 26.63 μmol L^{-1}) and **3f** (IC_{50} = 80.15 μmol L^{-1}) containing sulphonamide, methylthio-phenyl, 4-tosylphenyl, and (4-nitrophenyl)sulfonyl moiety, resp. The replacement of nitro (**3f**) with chloro (**3g**, IC_{50} = 45.72 μmol L^{-1}) causes a mild increase in inhibitory potency. The presence of *p*--hydroxy (**3h**, IC_{50} = 1.02 μmol L^{-1}) and *p*-methoxy (**3i**, IC_{50} = 1.45 μmol L^{-1}) group showed drastic improvement in the inhibitory potency. However, upon the introduction of *p*-fluoro (**3j**, IC_{50} = 67.13 μmol L^{-1}), the activity was found to be markedly reduced. None of the synthesized compounds showed better activity than dexamethasone (IC_{50} = 0.90 μmol L^{-1}) as the standard; however, compound **3h** showed the highest inhibitory activity amongst the tested derivatives on NF-κB transcription activity comparable to that of dexamethasone.

Moreover, SAR of compounds **3a-j** based on the NF-κB inhibitory activity suggests that phenyl-substituted sulphonamide derivatives (**3e**, **3f**, **3g**, **3h**, **3i,** and **3j**) exert a diverse range of inhibitory activity. Among them, compounds containing electron-withdrawing substituents (**3f**, **3g,** and **3j**) showed reduced inhibitory potency compared to those with electron-donating groups (**3e**, **3h,** and **3i**). Moreover, significant

Table III. In vitro *inhibitory effect of compounds **3a–j** on NF-κB transcriptional activity in LPS-stimulated RAW264.7 cells*[a]

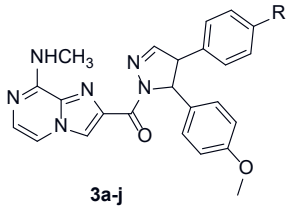

3a-j

Compd.	R	IC_{50} (μmol L^{-1})[a]	Compd.	R	IC_{50} (μmol L^{-1})[a]
3a		94.02 ± 11.86	**3f**	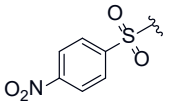	80.15 ± 7.30
3b		2.67 ± 1.02	**3g**	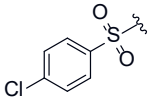	45.72 ± 4.30
3c		7.34 ± 1.43	**3h**	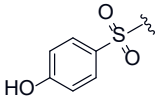	1.02 ± 0.29
3d		15.02 ± 2.23	**3i**	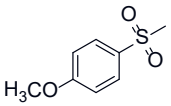	1.45 ± 0.38
3e	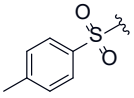	26.63 ± 2.62	**3j**	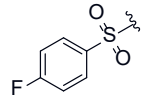	67.13 ± 7.23
Dexamethasone (reference)		0.90 ± 0.21			

[a] Mean ± SD of at least six independent assays.

inhibitory potency was observed in the case of compounds containing methyl sulphonyl (**3b**) and sulphonamide (**3c**) as substituents. The lowest inhibitory potency was observed for the compound containing the trifluoromethyl group (**3a**).

Pharmacology and toxicology

*Effect of compound **3h** on the viability of MCF-12A*. – The effect of compound **3h** on the viability of MCF-12A was evaluated first, where it showed no inhibitory effect at the maximum tested dose of 500 μmol L^{-1} as per the previously reported procedure (21). Thus, it could be corroborated that compound **3h** was non-toxic to normal epithelial cells.

*Acute oral toxicity of compound **3h***. – The acute oral toxicity of compound **3h** was also tested using the OECD method (22). The results suggested that compound **3h** did not show any toxic signs in the SD rat till the maximum tested dose of 2000 mg kg^{-1}. The toxic signs include changes in skin and fur, eyes, and mucous membranes, as well as respiratory, circulatory, autonomic, and central nervous systems, including changes in somatomotor activity and behavior patterns. Furthermore, tremors, convulsions, salivation, diarrhea, lethargy, sleep, and coma were also not observed.

*Effect of compound **3h** on the lung injury sepsis model in rat*. – Prompted by the inhibitory activity of compound **3h** on NF-κB transcription activity, and non-toxicity it is worthwhile to assess its effect on the sepsis-induced lung injury model in SD rats in reference to dexamethasone as standard. After establishing the lung injury sepsis model, the compound **3h** was administered to the experimental animals. The pharmacological benefit of compound **3h** was initially assessed by gross examination of lung histopathology of rats by H and E staining. As shown in Fig. 1a, as believed, the lung tissues were found normal in the sham group. In contrast, group 2 rats showed severe pathological changes, which were found to be totally different from the typical architecture. It revealed increased membrane permeability due to membrane damage caused by edema, fluid exudation, and a massive influx of inflammatory cells. Moreover, these pathological features were found restored near to normal in the compound **3h**-treated group with maximum benefit seen in group 4 (10 mg kg^{-1}) treated rats. The improvement in histopathology of the lung by compound **3h** at the dose of 10 mg kg^{-1} was found similar to the Dex-treated group. Studies have shown that lung injury induces vascular permeability, increasing the influx of protein-rich edema fluid in the lung (24, 25). Therefore, next, we aimed to determine the difference between the ratio of wet (W) to dry (D) mass of the lungs. This particular ratio is a well-established parameter to assess edema in the lungs and the rate of fluid filtration across the lung

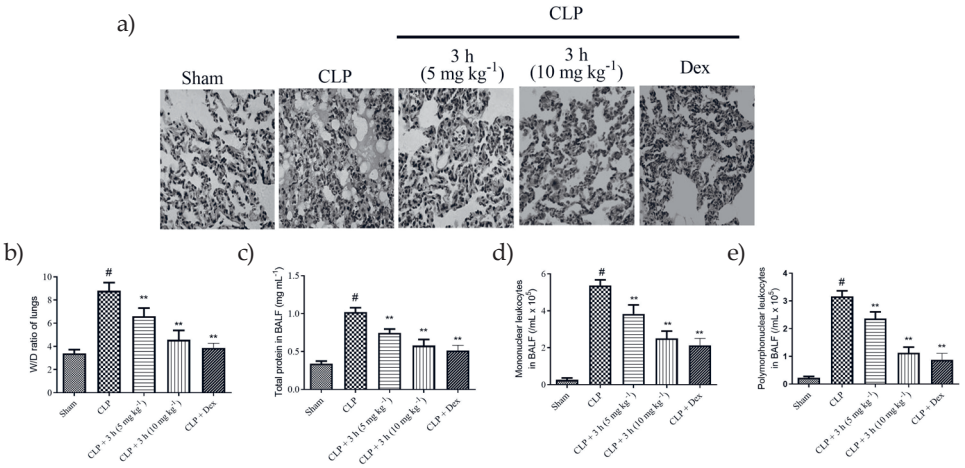

Fig. 1. Effect of compound **3h** on: a) histopathology of lung tissues in CLP rats; b) W/D ratio of lungs; c) total proteins in BALF; d) mononuclear leukocytes in BALF; e) poly-morphonuclear leukocytes in BALF. Values represent the mean ± SEM (n = 6). Statistically significant difference: $^{\#}p < 0.05$ *vs.* sham, $^{**}p < 0.05$ *vs*. CLP.

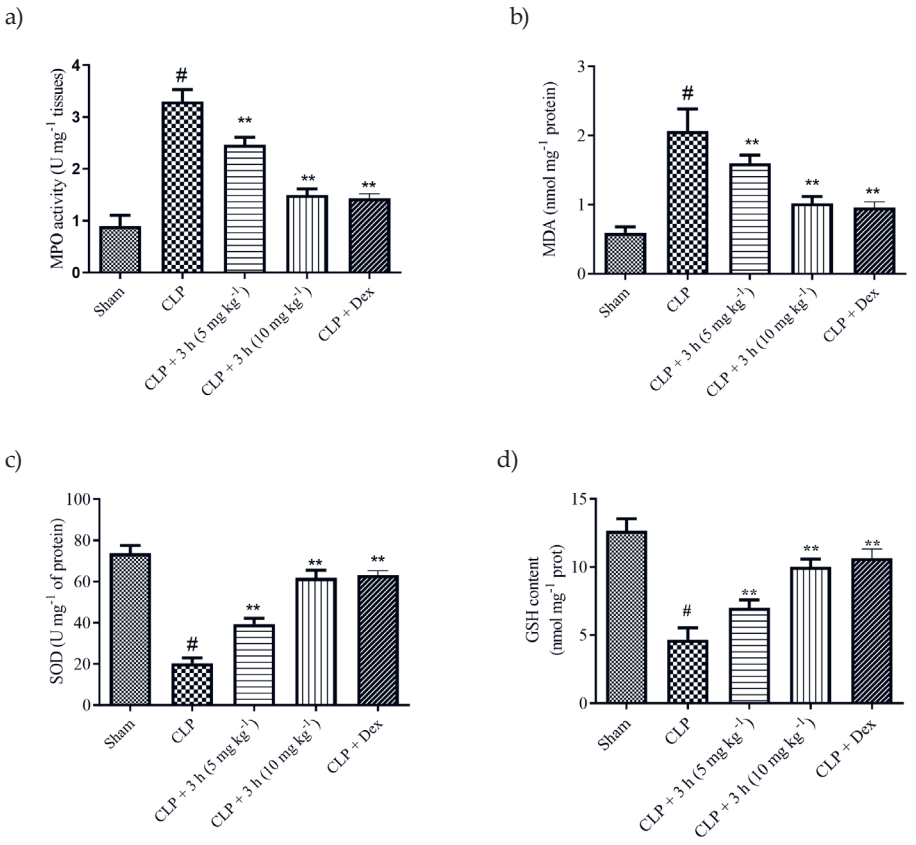

Fig. 2. Effects of compound **3h** on various biomarkers of oxidative stress in lungs in CLP rats: a) MPO; b) MDA; c) SOD; d) GSH. Values represent the mean ± SEM (n = 6). Statistically significant difference: $^{\#}p < 0.05$ *vs.* sham, $^{**}p < 0.05$ *vs.* CLP.

capillaries. The above results suggest that compound **3h** exerted a protective effect against lung injury in rats. The reduction of the W/D ratio of lung mass was found comparable to that of Dex as standard (Fig. 1b).

In the subsequent study, the effect of compound **3h** on the number of leukocytes and total proteins in the BALFs after CLP was examined. Various clinical studies have found significantly increased concentrations of total proteins and leukocytes in the lungs following the injury (26–29). As shown in Fig. 1c–e the concentration of total proteins, mononuclear leukocytes, and polymorphonuclear leukocytes was significantly increased in group 2 as compared to group 1 sham rats, whereas in compound **3h-**treated groups, the level of these biomarkers was found significantly restored near to the sham group values; this effect was found comparable to the Dex-treated group.

The excessive production of reactive species and free radicals leads to oxidative stress and studies showed that it has a significant role in the pathogenesis of sepsis-induced

injury (30, 31). A growing body of evidence suggests that antioxidants significantly benefit sepsis and represent a therapeutic strategy for sepsis-induced injury in septic patients (32–35). Therefore, the pharmacological effect of compound **3h** was evaluated on various oxidative stress biomarkers (MPO, MDA, SOD, and GSH), and results have been presented in Fig. 2. Myeloperoxidase (MPO) is a heme enzyme found in granules of the human inflammatory cells. Its increased level signifies generating reactive oxygen species (ROS), which modifies lipids, lipoproteins, and proteins in various disease states, including sepsis (36). Moreover, MDA is another biomarker that signifies the level of lipid peroxidation. A high MDA level in the disease state directly correlates with an increased level of lipid peroxidation due to an impaired oxidant defense mechanism (37). As shown in Fig. 2a,b the concentrations of MPO and MDA, were significantly higher in the CLP group compared to the sham but were reduced considerably in compound **3h**-treated rats. SOD and GSH are important antioxidants and are well known for their antioxidant nature by scavenging reactive free radicals. In sepsis or a disease state, these biomarkers are significantly reduced, which directly hamper the body's ability to clear off free radicals (38, 39). In the present study, compound **3h** significantly upregulated SOD and GSH. Thus, the results suggest that **3h** improves the antioxidant status of experimental rats.

Studies have shown that sepsis induces cellular damage, which recruits and activates innate immune cells. This activates Kupffer cells and promotes secretion of TNF-α, IL-1β, and IL-6 cytokines, which is an indicator of both oxidative stress and inflammatory reaction (40). The concentration of TNF-α, IL-1β, and IL-6 markedly increased in the CLP-treated group as compared to the sham (Fig. 3). Compound **3h**-treated rats showed a significant reduction in the elevated level of these cytokines which signifies anti-inflammatory activity of compound **3h**. The effects of compound **3h** in the dose of 10 mg kg^{-1} on oxidative stress biomarkers and pro-inflammatory cytokines was found.

Therefore, lastly, we have determined the effect of compound **3h** on the nuclear protein expression of NF-κB. NF-κB is considered a key signaling molecule responsible for the development and progression of inflammation in sepsis-induced injury. As a result, its inhibition showed significant benefits by reducing the level of acute inflammation and can then be able to prevent organ dysfunction (18). As shown in Fig. 4, compound **3h** significantly reduced the elevated level of nuclear NF-κB as compared to the CLP group in Western blot analysis. The results suggest that compound **3h** exerts a significant anti-inflammatory effect in CLP rats *via* inhibiting nuclear translocation and activation of NF-κB, which prevents inflammation and associated organ lung damage in sepsis rats.

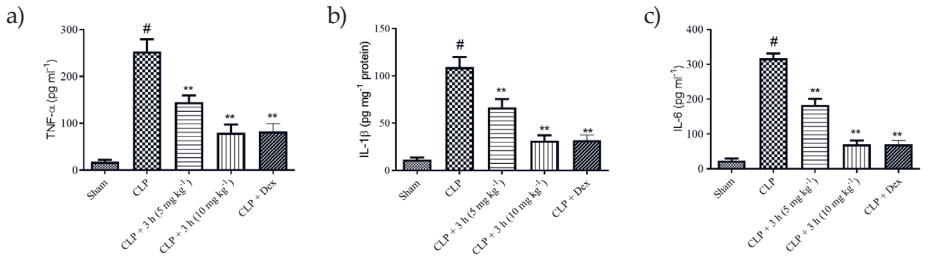

Fig. 3. Effects of compound **3h** on the expression of various pro-inflammatory cytokines in experimental animals: a) TNF-α, b) IL-1β, c) IL-6. Values represent the mean ± SEM (n = 6). Statistically significant difference: $^{\#}p < 0.05$ *vs.* sham, $^{**}p < 0.05$ *vs*. CLP.

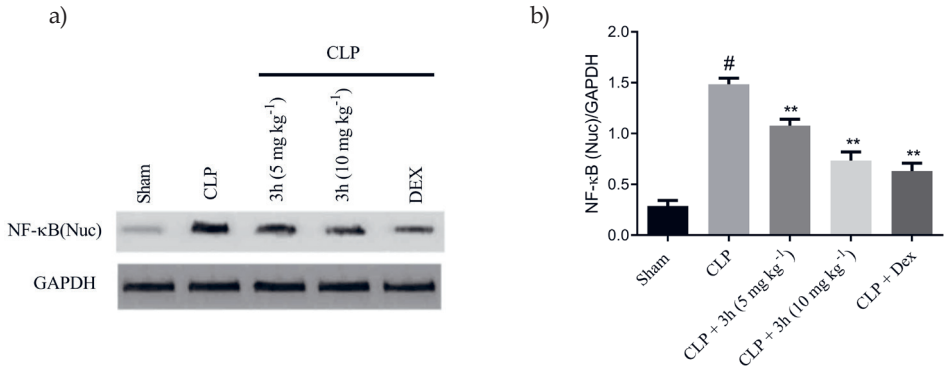

Fig. 4. Effect of compound **3h** on: a) nuclear NF-κB [NF-κB(nuc)] in CLP rats by Western blot analysis; b) semiquantitative analysis of NF-κB(nuc). Values represent the mean ± SEM (n = 6). Statistically significant difference: $^{\#}p < 0.05$ *vs.* sham, $^{**}p < 0.05$ *vs.* CLP.

Apoptosis, or programmed cell death, is an essential physiological process for developing and maintaining tissue homeostasis, ensuring a balance between cellular proliferation and turnover in nearly all tissue types (41). Accumulating evidence supports the impor-

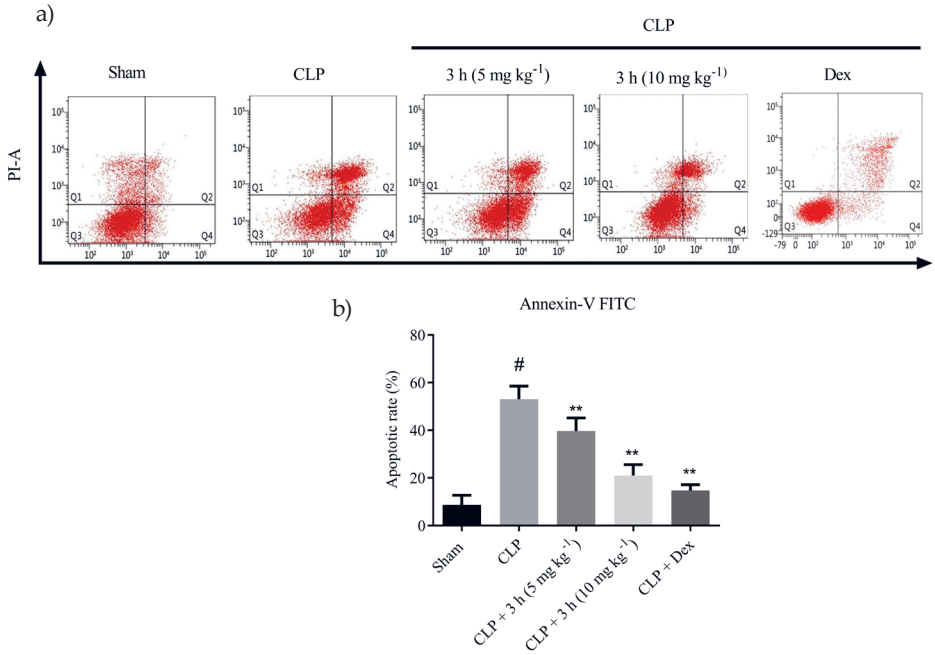

Fig. 5. Effect of compound **3h** on apoptosis in sepsis-mediated lung damage in CLP rats: a) flow cytometry detection, b) quantitative comparative analysis. Values represent the mean ± SEM (n = 6). Statistically significant difference: $^{\#}p < 0.05$ *vs.* sham, $^{**}p < 0.05$ *vs.* CLP.

tance of apoptosis as a potential pathogenic mechanism in the progression of sepsis-induced lung injury, and anti-apoptotic agents found as effective treatment therapy (42–44). Moreover, we have also analyzed the effect of compound **3h** on the apoptosis of the lung tissues using flow cytometry. As shown in Fig. 5, the sham-treated group showed no signs of apoptosis, whereas the rate of apoptosis was found significantly higher in CLP treated group as compared to the control. However, the percentage of cellular apoptosis was found significantly reduced in the compound **3h**-treated group, with maximum reduction achieved in the case of 10 mg kg^{-1} treated group. The pharmacological activity of Dex against apoptosis was found slightly superior.

CONCLUSIONS

ALI is a major cause of acute respiratory failure in patients with no effective treatment. Therefore, our study demonstrated the development of a novel class of pyrazole-conjugated imidazo[1,2-*a*]pyrazine derivatives against ALI. The results suggested that these derivatives showed considerable inhibition of NF-κB transcription activity. Among them, compound **3h** ((4-(4-((4-hydroxyphenyl)sulfonyl)phenyl)-5-(4-methoxyphenyl)-4,5-dihydro-1*H*-pyrazol-1-yl)(8-(methylamino)imidazo[1,2-*a*]pyrazin-2-yl)methanone), was identified as the most potent inhibitor. Compound **3h** showed a protective effect in SD rats against sepsis induced by the CLP method. Compound **3h** caused a significant reduction in lung edema and total proteins, mononuclear leukocytes, and polymorphonuclear leukocytes in BALF. The levels of oxidative stress and inflammation were also found significantly reduced in sepsis rats after treatment with compound **3h**. It showed a significant reduction in the apoptosis of lung tissues which was confirmed by histopathological changes observed in compound **3h**-treated lungs. Taken together, our results indicate compound **3h** as a potential lead molecule for the treatment of ALI.

Supplementary materials are available upon request.

Acronyms. – ALI – acute lung injury, ARDS – acute respiratory distress syndrome, CLP – cecal ligation puncture, DMEM – Dulbecco's modified Eagle's medium, FBS – fetal bovine serum, GAPDH – glyceraldehyde 3-phosphate dehydrogenase, GSH – glutathione, HRP – horseradish peroxidase, MDA – malondialdehyde, MPO – myeloperoxidase, MTT assay – 3-[4,5-dimethylthiazol-2-yl]-2,5 diphenyl tetrazolium bromide assay, NF-κB – nuclear factor kappa B, PVDF – polyvinylidene fluoride, SAR – structure-activity relationship, SDS-PAGE – sodium dodecyl sulphate-polyacrylamide gel electrophoresis, SOD – superoxide dismutase, TLR – toll-like receptor, TNF-α – tumor necrosis factor α, W/D – wet to dry.

Acknowledgements. – The authors are thankful to the Emergency Department, Henan Province Hospital of TCM, The Second Affiliated Hospital of the Henan University of TCM, Zhengzhou City for providing the facility to carry out the research work.

Conflict of interest. – Authors declare no conflict of interest.

Authors contributions. – BZ: Conceptualization, methodology, supervision, investigation, writing, original draft preparation, review, editing, LW: methodology, analysis, investigation, writing, original draft preparation. The authors have read and agreed to the published version of the manuscript.

REFERENCES

1. Y. Lin, Y. Xu and Z. Zhang, Sepsis-induced myocardial dysfunction (SIMD): the pathophysiological mechanisms and therapeutic strategies targeting mitochondria, *Inflammation* **43**(4) (2016) 1184–1200; https://doi.org/10.1007/s10753-020-01233-w
2. J. C. Marshall and A. al Naqbi, Principles of source control in the management of sepsis, *Crit. Care Clin.* **25**(4) (2019) 753–768; https://doi.org/10.1016/j.ccc.2009.08.001
3. E. R. Johnson and M. A. Matthay, Acute lung injury: Epidemiology, pathogenesis, and treatment, *J. Aerosol Med. Pulm. Drug Deliv.* **23**(4) 2010 243–252; https://doi.org/10.1089/jamp.2009.0775
4. Y. Chen, H. Tong, Z. Pan, D. Jiang, X. Zhang, J. Qiu, L. Su and M. Zhang, Xuebijing injection attenuates pulmonary injury by reducing oxidative stress and pro-inflammatory damage in rats with heat stroke, *Exp. Ther. Med.* **13** (2017) 3408–3416; https://doi.org/10.3892/etm.2017.4444
5. S. Saharan, R. Lodha and S. K. Kabra, Management of acute lung injury/ARDS, *Indian J. Pediatr.* 77(11) (2010) 1296–1302; https://doi.org/10.1007/s12098-010-0169-z
6. J. C. Rudkowski, E. Barreiro, R. Harfouche, P. Goldberg, O. Kishta, P. D'Orleans-Juste, J. Labonte, O. Lesur and S. N. A. Hussain, Roles of iNOS and nNOS in sepsis-induced pulmonary apoptosis, *Am. J. Physiol. Lung Cell. Mol. Physiol.* **286** (2004) L793–L800; https://doi.org/10.1152/ajplung.00266.2003
7. A. Ansari, A. Ali, M. Asif and Shamsuzzaman, Review: biologically active pyrazole derivatives, *New J. Chem.* **41** (2017) 16–41; https://doi.org/10.1039/c6nj03181a
8. J. Marino, *Celecoxib*, in *The Essence Analgesia and Analgesics* – Section 4 NSAIDS – Chapter 56, (Eds. R. S. Sinatra, J. S. Jahr and J. M. Watkins-Pitchford), Cambridge University Press, Cambridge 2010, pp. 238–242; https://doi.org/10.1017/CBO9780511841378.056
9. G. Steinbach, P. M. Lynch, R. K. S. Phillips, M. H. Wallace, E. Hawk, G. B. Gordon, N. Wakabayashi, B. Saunders, Y. Shen, T. Fujimura, L. K. Su, B. Levin, L. Godio, S. Patterson, M. A. Rodriguez-Bigas, S. L. Jester, K. L. King, M. Schumacher, J. Abbruzzese, R. N. DuBois, W. N. Hittelman, S. Zimmerman, J. W. Sherman and G. Kelloff, The effect of celecoxib, a cyclooxygenase-2 inhibitor, in familial adenomatous polyposis, *N. Engl. J. Med.* **342** (2000) 1946–1952; https://doi.org/10.1056/NEJM200006293422603
10. M. Mantzanidou, E. Pontiki and D. Hadjipavlou-Litina, Pyrazoles and pyrazolines as anti-inflammatory agents, *Molecules* **26**(11) (2021) Article ID 3439 (18 pages); https://doi.org/10.3390/molecules26113439
11. A. Rahman and F. Fazal, Blocking NF-kB: An inflammatory issue, *Proc. Am. Thorac. Soc.* **8**(6) (2011) 497–503; https://doi.org/10.1513/pats.201101-009MW
12. E. Abraham, Nuclear factor-κB and its role in sepsis-associated organ failure, *J. Infect. Dis.* **187** (2003) S364–S369; https://doi.org/10.1086/374750
13. C. Bhan, P. Dipankar, P. Chakraborty and P. P. Sarangi, Role of cellular events in the pathophysiology of sepsis, *Inflamm. Res.* **65**(11) (2016) 853–868; https://doi.org/10.1007/s00011-016-0970-x
14. L. Bird, Inflammation: Hope for sepsis treatment, *Nat. Rev. Drug Discov.* **9** (2010) 516–517; https://doi.org/10.1038/nrd3212
15. R. Goel, V. Luxami and K. Paul, Recent advances in development of imidazo[1,2-*a*]pyrazines: Synthesis, reactivity and their biological applications, *Org. Biomol. Chem.* **13**(12) (2015) 3525–3555; https://doi.org/10.1039/c4ob01380h
16. S. Hemasrilatha, K. Sruthi, A. Manjula, V. Harinadha Babu and B. Vittal Rao, Synthesis and anti-inflammatory activity of imidazo[1,2-*a*]pyridinyl/pyrazinyl benzamides and acetamides, *Indian J. Chem. – Sect. B Org. Med. Chem.* **51** (2012) 981–987.
17. A. Özdemir, G. Turan-Zitouni, Z. A. Kaplancikli and Y. Tunali, Synthesis and biological activities of new hydrazide derivatives, *J. Enzyme Inhib. Med. Chem.* **24** (2009) 825–831; https://doi.org/10.1080/14756360802399712

18. S. A. H. El-Feky, Z. K. Abd El-Samii, N. A. Osman, J. Lashine, M. A. Kamel and H. K. Thabet, Synthesis, molecular docking and anti-inflammatory screening of novel quinoline incorporated pyrazole derivatives using the Pfitzinger reaction II, *Bioorg. Chem.* **58** (2015) 104–116; https://doi.org/10.1016/j.bioorg.2014.12.003
19. J. K. Srivastava, G. G. Pillai, H. R. Bhat, A. Verma and U. P. Singh, Design and discovery of novel monastrol-1,3,5-triazines as potent anti-breast cancer agent *via* attenuating epidermal growth factor receptor tyrosine kinase, *Sci. Rep.* **7** (2017) Article ID 5851 (17 pages); https://doi.org/10.1038/s41598-017-05934-5
20. J. K. Srivastava, N. T. Awatade, H. R. Bhat, A. Kmit, K. Mendes, M. Ramos, M. D. Amaral and U. P. Singh, Pharmacological evaluation of hybrid thiazolidin-4-one-1,3,5-triazines for NF-κB, biofilm and CFTR activity, *RSC Adv.* **5**(108) (2015) 88710–88718; https://doi.org/10.1039/c5ra09250g
21. A. Masih, A. K. Agnihotri, J. K. Srivastava, N. Pandey, H. R. Bhat and U. P. Singh, Discovery of novel pyrazole derivatives as a potent anti-inflammatory agent in RAW264.7 cells via inhibition of NF-κB for possible benefit against SARS-CoV-2, *J. Biochem. Mol. Toxicol.* **35** (2021) e22656; https://doi.org/10.1002/jbt.22656
22. Organisation for Economic Co-operation and Development, *OECD Guidelines, OECD 423. Acute Oral Toxicity, OECD Guidelines for the Testing of Chemicals, Section 4*, OECD Publishing, Paris 2002; https://www.oecd-ilibrary.org/environment/test-no-423-acute-oral-toxicity-acute-toxic-class-method_9789264071001-en
23. L. Dejager, I. Pinheiro, E. Dejonckheere and C. Libert, Cecal ligation and puncture: The gold standard model for polymicrobial sepsis?, *Trends Microbiol.* **19**(4) (2011) 198–208; https://doi.org/10.1016/j.tim.2011.01.001
24. L. A. Huppert, M. A. Matthay and L. B. Ware, Pathogenesis of acute respiratory distress syndrome, *Semin. Respir. Crit. Care Med.* **40** (2019) 31–39; https://doi.org/10.1055/s-0039-1683996
25. A. J. Walkey, R. Summer, V. Ho and P. Alkana, Acute respiratory distress syndrome: Epidemiology and management approaches, *Clin. Epidemiol.* **4**(1) (2012) 159–169; https://doi.org/10.2147/CLEP.S28800
26. Q. Kong, X. Wu, Z. Qiu, Q. Huang, Z. Xia and X. Song, Protective effect of dexmedetomidine on acute lung injury via the upregulation of tumour necrosis factor-α-induced protein-8-like 2 in septic mice, *Inflammation* **43** (2020) 833–846; https://doi.org/10.1007/s10753-019-01169-w
27. M. T. P. de Oliveira, D. de S. Coutinho, É. T. de Souza, S. S. Guterres, A. R. Pohlmann, P. M. R. Silva, M. A. Martins and A. Bernardi, Orally delivered resveratrol-loaded lipid-core nanocapsules ameliorate LPS-induced acute lung injury via the ERK and PI3K/Akt pathways, *Int. J. Nanomed.* **14** (2019) 5215–5228; https://doi.org/10.2147/IJN.S200666
28. B. B. Davis, Y.-H. Shen, D. J. Tancredi, V. Flores, R. P. Davis and K. E. Pinkerton, Leukocytes are recruited through the bronchial circulation to the lung in a spontaneously hypertensive rat model of COPD, *PLoS ONE* **7**(3) (2012) e33304; https://doi.org/10.1371/journal.pone.0033304
29. J. Rebetz, J. W. Semple and R. Kapur, The pathogenic involvement of neutrophils in acute respiratory distress syndrome and transfusion-related acute lung injury, *Transfus. Med. Hemother.* **45**(5) (2018) 290–298; https://doi.org/10.1159/000492950
30. C. W. Chow, M. T. H. Abreu, T. Suzuki and G. P. Downey, Oxidative stress and acute lung injury, *Am. J. Respir. Cell Mol. Biol.* **29**(4) (2003) 427–431; https://doi.org/10.1165/rcmb.F278
31. H. S. Park, S. R. Kim and Y. C. Lee, Impact of oxidative stress on lung diseases, *Respirology* **14**(1) (2009) 27–38; https://doi.org/10.1111/j.1440-1843.2008.01447.x
32. V. M. Victor, M. Rocha and M. De La Fuente, Immune cells: Free radicals and antioxidants in sepsis, *Int. Immunopharmacol.* **4**(3) (2004) 327–347; https://doi.org/10.1016/j.intimp.2004.01.020

33. D. Bin Yim, D. E. Lee, Y. So, C. Choi, W. Son, K. Jang, C. S. Yang and J. H. Kim, Sustainable nanosheet antioxidants for sepsis therapy via scavenging intracellular reactive oxygen and nitrogen species, *ACS Nano* **14** (2020) 10324–10336; https://doi.org/10.1021/acsnano.0c03807
34. H. F. Galley, Bench-to-bedside review: Targeting antioxidants to mitochondria in sepsis, *Crit. Care* **14**(4) (2010) Article ID 230 (9 pages); https://doi.org/10.1186/cc9098
35. M. Rocha, R. Herance, S. Rovira, A. Hernández-Mijares and V. M. Victor, Mitochondrial dysfunction and antioxidant therapy in sepsis, *Infect. Disord. - Drug Targets* **12**(2) (2012) 161–178; https://doi.org/10.2174/187152612800100189
36. A. Strzepa, K. A. Pritchard and B. N. Dittel, Myeloperoxidase: A new player in autoimmunity, *Cell. Immunol.* **317** (2017) 1–8; https://doi.org/10.1016/j.cellimm.2017.05.002
37. D. R. Janeiro, Malondialdehyde and thiobarbituric acid-reactivity as diagnostic indices of lipid peroxidation and peroxidative tissue injury, *Free Radic. Biol. Med.* **9**(6) (1990) 515–540; https://doi.org/10.1016/0891-5849(90)90131-2
38. J. Sha, B. Sui, X. Su, Q. Meng and C. Zhang, Alteration of oxidative stress and inflammatory cytokines induces apoptosis in diabetic nephropathy, *Mol. Med. Rep.* **16** (2017) 7715–7723; https://doi.org/10.3892/mmr.2017.7522
39. D. K. Gupta, J. M. Palma and F. J. Corpas (Eds.), *Reactive Oxygen Species and Oxidative Damage in Plants Under Stress*, Springer, Cham 2015.
40. R. B. Goodman, J. Pugin, J. S. Lee and M. A. Matthay, Cytokine-mediated inflammation in acute lung injury, *Cytokine Growth Factor Rev.* **14**(6) (2003) 523–535; https://doi.org/10.1016/S1359-6101(03)00059-5
41. U. P. Singh, J. K. Srivastava and H. R. Bhat, Discovery of novel 1,3,5-triazine-thiourea based dual PI3K/mTOR inhibitor against non-small cell lung cancer (NSCLC), *Ann. Oncol.* **27**(Suppl. 9) (2016) 161P - Abstracts ix50; https://doi.org/10.1016/S0923-7534(21)00319-7
42. Q, Kong, X. Wu, Z. Qiu, Q. Huang, Z. Xia and X. Song, Protective effect of dexmedetomidine on acute lung injury via the upregulation of tumour necrosis factor-α-induced protein-8-like 2 in septic mice, *Inflammation* **43** (2020) 833–846; https://doi.org/10.1007/s10753-019-01169-w
43. Y. Chen, H. Tong, Z. Pan, D. Jiang, X. Zhang, J. Qiu, L. Su and M. Zhang, Xuebijing injection attenuates pulmonary injury by reducing oxidative stress and pro-inflammatory damage in rats with heat stroke, *Exp. Ther. Med.* **13** (2017) 3408–3416; https://doi.org/10.3892/etm.2017.4444
44. D. Jiang, J. Liang, J. Fan, S. Yu, S. Chen, Y. Luo, G. D. Prestwich, M. M. Mascarenhas, H. G. Garg, D. A. Quinn, R. J. Homer, D. R. Goldstein, R. Bucala, P. J. Lee, R. Medzhitov and P. W. Noble, Regulation of lung injury and repair by toll-like receptors and hyaluronan, *Nat. Med.* **11** (2005) 1173–1179; https://doi.org/10.1038/nm1315